DDSPR: Dynamic Domain Selection and Pseudo-label Refinement for Cross-Subject EEG-based Emotion Recognition

Qinyu Hai (qyhai@stu.xidian.edu.cn)
Liying Yang* (yangliying1208@163.com)
Yumeng Ye (yeyumeng@stu.xidian.edu.cn)
Qiang Wang (qiang_wang@stu.xidian.edu.cn)
Jingtao Du (jtdu@stu.xidian.edu.cn)
Huanyu He (hyuhe@stu.xidian.edu.cn)
Department of Computer Science and
Technology, Xidian University, Xi'an, China

Abstract

Automatic emotion recognition using electroencephalography (EEG) signals has garnered significant attention in recent years. While multi-source domain adaptation methods provide a promising framework for cross-subject emotion recognition, the distributional discrepancies among different source domains often result in negative transfer. To address these challenges, we propose a two-stage Dynamic Domain Selection and Pseudo-label Refinement (DDSPR) model. In the first stage, we introduce a novel Dynamic Domain Selection (DDS) module and an Agent Domain Adaptation Strategy (ADAS) to dynamically identify and align source domains. In the second stage, a confidence-based pseudo-label correction strategy is employed to refine target domain labels and mitigate noise. We evaluate the proposed model through cross-subject experiments on the SEED and SEED-IV datasets, achieving accuracies of 91.50% ± 7.05 and 78.05% ± 13.56, respectively. The results demonstrate its effectiveness in emotion recognition performance.

Keywords: EEG; Emotion recognition; Multi-source domain adaptation; Domain selection

Introduction

Emotions serve as reflections of an individual's current physiological and psychological state, significantly influencing cognition, communication, and decision-making. Emotion, a fundamental indicator of human physiological and psychological states, profoundly shapes individual behavior, decision-making, and social interactions (Dolan, 2002). The process of emotion recognition involves inferring an individual's emotional state by analyzing physiological signals, including electroencephalograms (EEG). In recent years, EEG has attracted significant research interest due to its non-invasive nature, real-time monitoring capabilities, and sensitivity to emotional variations (Musha, Terasaki, Haque, & Ivamitsky, 1997) (Teplan et al., 2002). Despite these advantages, achieving accurate and efficient emotion recognition remains a key challenge in the field (Jayaram, Alamgir, Altun, Scholkopf, & Grosse-Wentrup, 2016).

Early studies on EEG-based emotion recognition predominantly employed handcrafted feature extraction combined with traditional machine learning methods, such as Support Vector Machines (SVM) and k-Nearest Neighbors (k-NN) (X.-W. Wang, Nie, & Lu, 2011; Rahman, Ghosh, Shuvo, & Rahman, 2015). While these approaches demonstrated initial success, they often assume fixed data distributions. Consequently, their performance deteriorates under substantial distributional shifts between source and target domains, posing significant challenges to cross-subject generalization.

To mitigate the challenges posed by cross-subject distributional differences, domain adaptation techniques have emerged as a prominent area of research (Yan, Kou, & Zhang, 2017). These methods are broadly categorized into single-source domain adaptation and multi-source domain adaptation, depending on the number of input domains utilized by the model.

In the domain of single-source domain adaptation (SSDA), Ganin et al. (Ganin et al., 2016) introduced an adversarial adaptation approach that leverages a minimax optimization strategy to learn domain-invariant features through the interplay of a feature extractor and a domain discriminator. While this method has shown promise, SSDA is inherently limited by its reliance on a single source domain. This constraint often hampers its ability to capture the full complexity of the target domain. Consequently, when there is a substantial distributional disparity between the source and target domains, the model's transfer performance tends to degrade.

Multi-source domain adaptation (MSDA) has emerged as a promising solution to address the limitations inherent in single-source domain adaptation (SSDA). By leveraging information from multiple source domains, MSDA enhances emotion recognition performance in the target domain by reducing bias associated with reliance on a single source domain and improving the model's generalization capabilities. For example, Wang et al. (F. Wang, Zhang, Xu, Ping, & Chu, 2021) proposed the use of domain-specific classifiers for each source domain, enabling the identification and alignment of the source domain most similar to the target domain. Similarly, Li et al. (J. Li, Qiu, Shen, Liu, & He, 2019) introduced a source domain selection strategy that identifies suitable existing datasets and applies style transfer mappings, thereby reducing the discrepancies in EEG feature distributions between source and target domains.

While multi-source domain adaptation (MSDA) methods have shown strong performance across various tasks, they are not without limitations. When all source domains are included in the training process, significant distributional differences among source domains can introduce noise, impeding effective feature alignment and compromising model stability (Salimnia, 2023). Additionally, conventional domain selection approaches often rely on fixed criteria to evaluate the

In D. Barner, N.R. Bramley, A. Ruggeri and C.M. Walker (Eds.), *Proceedings of the 47th Annual Conference of the Cognitive Science Society*

similarity between source and target domains. Such static selection strategies fail to account for the dynamic nature of target domain features, limiting their ability to adapt in real time and potentially reducing the effectiveness of domain alignment.

To address the aforementioned challenges, we present the Dynamic Domain Selection and Pseudo-label Refinement (DDSPR) model, which operates in two stages. In the first stage, the Dynamic Domain Selection (DDS) module employs a novel source domain selector based on central moment discrepancy (CMD) to dynamically identify and form combined source domains for adaptation. Building on this foundation, the Agent Domain Adaptation Strategy (ADAS) designates the most similar source domain as an agent target domain. By minimizing the maximum mean discrepancy (MMD) between the agent target domain and the remaining combined source domains, ADAS strengthens source domain consistency and improves domain selection efficiency. In the second stage, the label refinement module employs a confidence-based pseudo-label correction strategy to mitigate errors introduced by inaccurate pseudo-labels from the target domain. We validate the DDSPR model through leave-one-subject-out cross-validation on the SEED and SEED-IV datasets. The primary contributions and innovations of this work are summarized as follows:

- We propose a Dynamic Domain Selection (DDS) module leveraging central moment discrepancy (CMD), which effectively mitigates the impact of dissimilar source domains on the model's classification performance.
- We introduce an Agent Domain Adaptation Strategy (ADAS) as a complementary enhancement to the domain selection process, significantly improving the model's ability to adaptively select and align source domains.
- Our method is validated on the SEED and SEED-IV datasets, achieving superior emotion recognition performance compared to existing methods.

Method

Structure Overview

Our input comprises of M labeled source domains $\{S_m\}_{m=1}^{M}$ and an unlabeled target domain T. Each source domain S_m contains N_m labeled samples $(\mathrm{X}_{S_m}, \mathrm{Y}_{S_m}) = \{(\mathrm{x}_i, \mathrm{y}_i)\}_{i=1}^{N_m}$. The target domain T consists N_t unlabeled samples $\mathrm{X}_T = \{\mathrm{x}_j\}_{j=1}^{N_t}$. We use the labeling function G to represent a deep neural network model. The feature extractor G_f^{θ}, maps input data to feature representations, producing $\mathrm{z} = G_f(\mathrm{x};\theta_f)$. The architecture of G_f comprises two linear layers, each with an output dimension of 512. To improve the generalization and robustness of the feature extractor, Batch Normalization (BN), ReLU activation, and dropout are applied after each linear layer. Additionally, Gaussian noise is introduced between the two linear layers to mitigate overfitting. Following feature extraction, the features are normalized using L_2 normalization, projecting them onto a spherical space. For label prediction, we employ the label classifier G_h^{θ}, where $\hat{\mathrm{y}} = G_h(\mathrm{z};\theta_h)$. To generate pseudo-labels, we utilize Spherical Logistic Regression (SLR) (Salimnia, 2023) as the classifier. In the first stage of the model, θ_f represents the parameters of the feature extractor, and the two instances of the feature extractor, $G_{f_1}^{\theta}$ and $G_{f_2}^{\theta}$, share identical parameter configurations. Similarly, θ_h denotes the parameters of the label classifier in the first stage. In the second stage, the parameters of the feature extractor and label classifier are represented by ϕ_f and ϕ_h, respectively. Our objective is to dynamically select combined source domains in the first stage and then optimize the functions ϕ_f and ϕ_h in the second stage. This process enables the deep neural network G to accurately predict labels in the target domain, addressing domain shift and mitigating the negative transfer issues arising from domain misalignment.

Figure 1 illustrates the structure of the proposed DDSPR model, which is designed in two stages: the domain selection stage and the label rectification stage. During the first stage, a Dynamic Domain Selection (DDS) module is employed to identify the most relevant source domains. Simultaneously, the Agent Domain Adaptation Strategy (ADAS) is integrated to enhance the selection of combined source domains that are most similar to the target domain. In the subsequent label rectification stage, pseudo-labels for the target domain are corrected, and the feature distributions between the combined source domains and the target domain are aligned. Finally, the model's performance is evaluated based on predictions in the target domain. The following sections provide a comprehensive explanation of each component in detail.

Domain Selection Stage

One of the primary challenges in MSDA lies in addressing the distributional discrepancy between source and target domains. Significant differences between X_{S_m} and X_T can introduce noise, ultimately degrading the model's performance—a phenomenon known as negative transfer.To mitigate this issue, selecting the source domains X_{S_m} that closely align with the distribution of X_T reduces the adverse impact of dissimilarity. This approach effectively minimizes the likelihood of negative transfer, thereby enhancing the robustness of the adaptation process.

As illustrated in Figure 1, the pre-processed EEG features are first input into the feature extractor G_{f_1}, which generates the corresponding feature representations. These features are then passed to the dynamic domain selection (DDS) module, where the most relevant X_{S_m} are selected to form the combined source domains, denoted as $X_{S'}$. Subsequently, features are re-extracted from $X_{S'}$, and the label classifier is employed to generate pseudo-labels for the target domain. During this process, $G_{f_1}^{\theta}, G_{f_2}^{\theta}$,and G_h^{θ} are fine-tuned to optimize their performance. The final objective of this stage is to produce the refined combined source domains $X_{S'}^{D}$ and the determined pseudo-labels for the target domain, $\hat{Y}_T^{D}$.

Dynamic Domain Selection (DDS) Inspired by the domain correlation weighted moment distance (Zuo, Yao, & Xu,

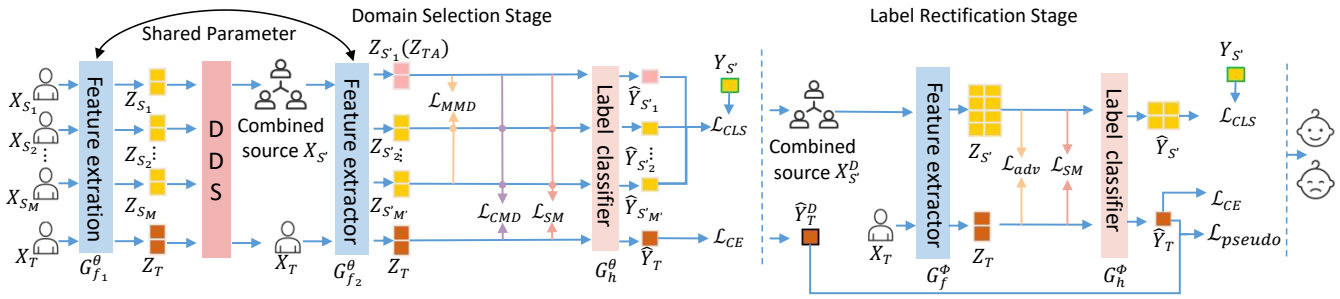

Figure 1: The architecture of DDSPR model. The entire model is primarily divided into two main modules: **(1) Domain selection stage**: Generate the combined source domains and the determined pseudo-labels for the target domain. **(2) Label rectification stage**: Correct incorrect target domain pseudo labels and evaluate the prediction results.

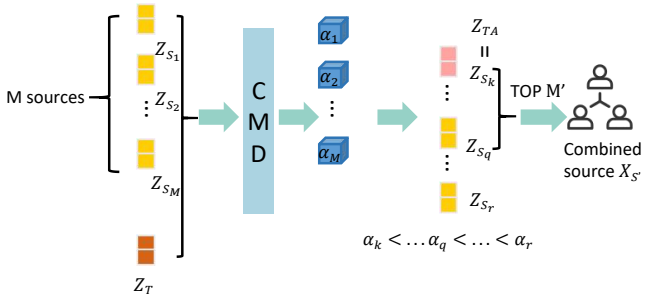

Figure 2: Dynamic domain selection module (DDS). Compare the discrepancy between different source domains to select combined source domains.

2021) , we propose a simplified and more efficient strategy to mitigate negative transfer. As shown in Figure 2, the discrepancy $\{\alpha_m\}_{m=1}^M$ between X_{S_m} and X_T is computed. A smaller discrepancy indicates greater similarity between the domains in their feature spaces. Subsequently, the top M' domains with the highest similarity to the target domain are selected, forming the combined source domains $X_{S'}$. The central moment discrepancy (CMD) (Xie, Zheng, Chen, & Chen, 2018a) is leveraged to quantify the discrepancy between the feature distributions of X_{S_m} and X_T. Initially, the positional discrepancy in the feature space is computed for X_{S_m} and X_T, represented as $\{\alpha'_m\}_{m=1}^M$, using the following equation:

$$\{\alpha'_m\}_{m=1}^M = \left\| \mathbb{E}(G_{f_1}^\theta(\mathrm{X}_{S_m})) - \mathbb{E}(G_{f_1}^\theta(\mathrm{X}_T)) \right\|_2 \quad (1)$$

The deeper-level discrepancy in the high-level statistics of X_{S_m} and X_T, denoted as $\{\alpha''_m\}_{m=1}^M$, is then calculated as follows:

$$\{\alpha''_{\mathrm{m}}\}_{\mathrm{m}=1}^{\mathrm{M}} = \sum_{k=2}^{K} \left\| B_k(G_{f_1}^\theta(\mathrm{X}_{S_m})) - B_k(G_{f_1}^\theta(\mathrm{X}_T)) \right\|_2 \quad (2)$$

where K is the maximum order of the central moments, while the term $B_k(\cdot)$ is the central moment of order k. By accumulating the higher-order central moments, we can obtain a deeper-level discrepancy between the source domain and the target domain in terms of their distributional shapes. The overall discrepancy is then computed as follows:

$$\{\alpha_m\}_{m=1}^M = \sum_{m=1}^{M} \alpha'_m + \alpha''_m \quad (3)$$

By sorting the above discrepancies, the similarity between the source domains and the target domain is derived:

$$\alpha_k < \cdots < \alpha_q < \cdots < \alpha_r \quad (4)$$

Finally, the top M' most similar source domains are selected based on the discrepancy to form the combined source domains $X_{S'}$.

Agent Domain Adaptation Strategy (ADAS) The dynamic domain selection (DDS) method mitigates negative transfer by selecting source domains similar to the target domain. However, it is often challenged by significant discrepancies among source domains, leading to transfer instability. To address this, we propose the Adaptive Domain Alignment Strategy (ADAS). First, the source domain with the smallest discrepancy α_{min} is selected as the agent target domain X_{TA}. The maximum mean discrepancy (MMD) (Gretton, Borgwardt, Rasch, Schölkopf, & Smola, 2012) between X_{TA} and the other combined source domains $X_{S''_m}$ is computed to enhance source domain alignment. This process improves domain consistency and indirectly boosts the model's transfer performance. The formulation is defined as:

$$\begin{aligned} \mathcal{L}_{\mathrm{MMD}} = \sum_{i=1}^{Q} \Big(& \left\| F_i(G_{f_2}^\theta(\mathrm{X}_{TA}), G_{f_2}^\theta(\mathrm{X}_{TA})) \right\| \\ & + \left\| F_i(G_{f_2}^\theta(\mathrm{X}_{S''_m}), G_{f_2}^\theta(\mathrm{X}_{S''_m})) \right\| \\ & - 2 \left\| F_i(G_{f_2}^\theta(\mathrm{X}_{TA}), G_{f_2}^\theta(\mathrm{X}_{S''_m})) \right\| \Big) \end{aligned} \quad (5)$$

where $F(\cdot)$ denotes the kernel matrix calculated using the multi-scale Gaussian kernel function, and Q represents the number of multi-scale Gaussians . Minimizing this loss aligns the feature distributions of X_{TA} and $X_{S''_m}$ thereby enhancing

the model's generalization and improving the DDS module's effectiveness in source domain selection and transfer performance.

Global Feature Alignment To enhance global alignment between the combined source domains $X_{S'}$ and the target domain, we employ classification loss $\mathcal{L}_{\text{cls}}$ (Goodfellow, Bengio, Courville, et al., 2016) to improve source domain classification performance and conditional entropy loss $\mathcal{L}_{\text{CE}}$ (Shu, Bui, Narui, & Ermon, 2018) to strengthen class separation in the target domain. The corresponding formulations are calculated as:

$$\mathcal{L}_{\text{cls}} = -\mathbb{E}_{\mathrm{x}_{S'},\mathrm{y}_{S'}\sim(\mathrm{X}_{S'},\mathrm{Y}_{S'})} \sum_{k=1}^{K} \mathbf{1}_{(k=y_{S'})} \log G_h^{\theta}(\mathrm{Z}_{S'}) \tag{6}$$

$$\mathcal{L}_{\text{CE}} = -\mathbb{E}\left[G_h^{\theta}(Z_T)^{\top} \ln G_h^{\theta}(Z_T)\right] \tag{7}$$

where $(\mathrm{X}_{S'},\mathrm{Y}_{S'})=\{\mathrm{X}_{S'm},\mathrm{Y}_{S'm}\}_{m=1}^{M'}$ denotes the set of all data in the combined source domains. K represents the total number of classes. 1 is an indicator function, which outputs 1 only when $G_h^{\theta}(\mathrm{Z}_{S'})$ matches class k. X_T is the set of unlabeled samples from the target domain, and $G_h^{\theta}(\mathrm{Z}_T)$ is the predicted distribution of the target domain samples.

Local Feature Alignment To enhance the model's generalization and fulfill the first-stage objectives, we incorporate semantic loss $\mathcal{L}_{\text{SM}}$ (Xie, Zheng, Chen, & Chen, 2018b) and central moment discrepancy loss $\mathcal{L}_{\text{CMD}}$ for localized feature alignment between $X_{S'}$ and X_T. Specifically, $\mathcal{L}_{\text{SM}}$ aligns the feature distributions of samples belonging to the same class across the source and target domains. This involves defining target domain classes using pseudo-labels and aligning class centroids across domains. The formulation is presented as:

$$\mathcal{L}_{\text{SM}} = \sum_{k=1}^{K} \text{dist}(C_{S'_m}^k, C_T^k) \tag{8}$$

where $C_{S'_m}^k$ and C_T^k denote the centroids of class k in $X_{S'}$ and X_T, respectively. Cosine distance is employed to quantify the similarity between these centroids, facilitating alignment of feature distributions within each class.

To achieve finer local alignment of individual sample feature distributions across domains, higher-order statistical moments are matched using the central moment discrepancy loss $\mathcal{L}_{\text{CMD}}$. This enhances the precision of cross-domain alignment. The formulation of $\mathcal{L}_{\text{CMD}}$ is as follows:

$$\begin{aligned}\mathcal{L}_{\text{CMD}} = &\parallel \mathbb{E}[G_{f_2}^{\theta}(\mathrm{X}_{S'_m})] - \mathbb{E}[G_{f_2}^{\theta}(\mathrm{X}_T)] \parallel_2 \\ &+ \sum_{k=2}^{K} \left\| B_k(G_{f_2}^{\theta}(\mathrm{X}_{S'_m})) - B_k(G_{f_2}^{\theta}(\mathrm{X}_T)) \right\|_2 \end{aligned} \tag{9}$$

Total loss Finally, the total loss in the domain selection stage is defined as:

$$\begin{aligned}\mathcal{L}_{\text{stage1}} = &\mathcal{L}_{\text{cls}} + \sigma_1 \mathcal{L}_{\text{CE}} + \sigma_2 \cdot \sum_{m=1}^{M'} \Big[\omega_{\text{CMD}}^{(m)} \cdot \mathcal{L}_{\text{CMD}} \\ &+ \omega_{\text{SM}}^{(m)} \cdot \mathcal{L}_{\text{SM}}\Big] + \sigma_3 \mathcal{L}_{\text{MMD}} \end{aligned} \tag{10}$$

In this total loss,the parameters σ_1, σ_2 and σ_3 are used to control the importance weights of different components. $\omega_{\text{CMD}}^{(\text{m})}$ and $\omega_{\text{CMD}}^{(\text{m})}$ are dynamic weights used to measure the relevance of the m-th source domain to the target domain. These weights are defined as follows:

$$a_m = \frac{1}{\mathcal{L}_{\text{CMD}}} \quad \text{and} \quad \omega_{\text{CMD}}^{(m)} = \frac{\exp(a_m)}{\sum_{j=1}^{M'} \exp(a_j)} \tag{11}$$

where a_m and a_j represent the adaptability of the m-th and j-th selected source domains.

Label Rectification Stage

In the domain selection stage, the Dynamic Domain Selection (DDS) module and the Agent Domain Adaptation Strategy (ADAS) are utilized to mitigate the impact of dissimilar source domains and identify the combined source domains. Following this, the neural network G trained in the first stage predicts pseudo-labels for X_T, denoted as $\hat{Y}_T^D$. Simultaneously, the combined source domains from the final iteration of the first stage are fixed as $X_{S'}^D$. Feed both into the next stage for pseudo-label correction and evaluate the prediction results.

Pseudo-label Correction During the domain adaptation process, the model relies heavily on pseudo-labels for training. However, due to distributional discrepancies between the source and target domains, these pseudo-labels may include considerable noise. Since the primary objective of the first stage is to identify the most similar combined source domains $X_{S'}^D$, incorporating label rectification at this stage could potentially divert the model's optimization trajectory and degrade performance. To address this, pseudo-label correction is implemented in the second stage to filter and enhance the quality of pseudo-labels, thereby mitigating the adverse effects of erroneous labels and improving overall model robustness.

A pseudo-label correction loss, $\mathcal{L}_{\text{pse}}$ (Gu, Sun, & Xu, 2020), is employed to enhance the utilization efficiency of pseudo-labeled samples from the target domain. This approach dynamically adjusts the contribution weights of pseudo-labeled samples to the loss function by incorporating the confidence scores associated with these samples. Specifically, the loss is calculated as:

$$\mathcal{L}_{\text{pse}} = \frac{1}{N_0} \Sigma_{j=1}^{N_T} \omega_{\Phi}(X_{T_j}) \mathcal{J}(\widehat{Y}_{T_j}, \widehat{Y}_{T_j}^D) \tag{12}$$

where $N_0 = \sum_{j=1}^{N_T} \omega_{\Phi}(\mathrm{X}_{T_j})$ is a normalization factor used to balance the sum of the weights. $\mathcal{J}(\widehat{\mathrm{Y}}_{T_j}, \widehat{\mathrm{Y}}_{T_j}^D)$ is the classification error of the pseudo-labeled samples, where the Mean

Absolute Error (MAE) is used as the metric. The weight of the pseudo-labeled samples $\omega_\Phi(X_{T_j})$ is determined by the following rule:

$$\omega_\Phi(X_{T_j}) = \begin{cases} \varphi_j & \text{if } \varphi_j \geq 0.5, \\ 0 & \text{otherwise} \end{cases} \tag{13}$$

where $\varphi_j = P_\Phi(z_j = 1|\mathrm{X_{T_j}}, \hat{\mathrm{Y}}_{\mathrm{T_j}}).z_j \in 0, 1$ is a random variable of each pseudo-labeled sample to indicate the probability that the pseudo-labeled sample is correctly labeled. The probability φ_j is estimated using a Gaussian mixture model P_ϕ. According to the model, the distribution is estimated based on the distance of the feature sample from the class center. When φ_j<0.5 the sample is considered to have low confidence, and its contribution to the loss is reduced.

Adversarial Training The adversarial module in the Domain-Adversarial Neural Network (DANN) (Zeng et al., 2021) is used for adversarial training, with the aim of aligning the features of $X_{S'}^{\mathrm{D}}$ and X_T, thereby further reducing the risk of negative transfer. The adversarial loss $\mathcal{L}_{\text{adv}}$ is defined as follows:

$$\mathcal{L}_{\text{adv}} = -\mathbb{E}[\log \mathcal{D}(G_f^\phi(\mathrm{X}_{S'}^{\mathrm{D}}))] - \mathbb{E}[\log(1 - \mathcal{D}(G_f^\phi(\mathrm{X}_T)))] \tag{14}$$

where $D(\cdot)$ represents the domain discriminator, which determines whether the input feature originates from the source domains (output = 1) or the target domain (output = 0). By leveraging the adversarial loss $\mathcal{L}_{\text{adv}}$, the model's cross-domain transfer capability is significantly enhanced at this stage, thereby effectively improving classification performance on the target domain.

Total loss The total loss of label rectification stage is:

$$\mathcal{L}_{\text{stage2}} = \mathcal{L}_{\text{adv}} + \mathcal{L}_{\text{pse}} + \mathcal{L}_{\text{cls}} + \rho_1 \mathcal{L}_{\text{CE}} + \rho_2 \mathcal{L}_{\text{SM}} \tag{15}$$

In this loss, $\mathcal{L}_{\text{stage2}}$, the global losses $\mathcal{L}_{\text{cls}}$ and $\mathcal{L}_{\text{CE}}$ are employed to maintain the model's classification capability across both source and target domains. Simultaneously, $\mathcal{L}_{\text{SM}}$ is applied to minimize domain discrepancies at the category level. Additionally, ρ_1 and ρ_2 serve as importance weights to balance the contributions of the respective components. By optimizing this total loss, pseudo-label correction is achieved, thereby completing the emotion recognition task.

EXPERIMENTS

Datasets and Data Processing

The experiments utilize two widely used publicly available EEG emotion recognition datasets, SEED and SEED-IV. The SEED dataset (Zheng & Lu, 2015) includes EEG signals from 15 subjects induced into positive, neutral, and negative emotions by watching 15 four-minute Chinese movie clips. Data is sampled at 1 kHz across three sessions over one week, yielding 45 trials per subject. The SEED-IV dataset (Zheng, Liu, Lu, Lu, & Cichocki, 2018) comprises EEG recordings from 15 subjects exposed to 2-minute movie clips designed to evoke four emotions: happiness, sadness, neutral, and fear. Each subject completed 24 trials across three sessions.

In this study, the differential entropy (DE) features provided by the SEED and SEED-IV datasets are utilized. The raw EEG signals are resampled to 200 Hz and band-pass filtered (1–75 Hz). SEED and SEED-IV data are segmented into 1-second and 4-second intervals, respectively, and DE features are extracted across five frequency bands: delta, theta, alpha, beta, and gamma. For each subject, the feature dimensions are "62 channels × number of trials × 5 frequency bands", totaling 310 dimensions. In the SEED dataset, DE features extracted per second are concatenated into time windows. Each window spans 9 seconds, with an overlap of 8 seconds between consecutive windows (Yang & Liu, 2019). This process yields 2655 samples per trial, with each sample comprising 9 time windows × 310 features and corresponding labels. For the SEED-IV dataset, we enhance feature complementarity by applying two smoothing methods: linear dynamic systems and moving averages (Bashivan, Rish, Yeasin, & Codella, 2015). The resulting data dimensions for SEED-IV are 851/832/822 samples × 620 features (310 × 2 smoothing types).

Implementation Details

In the DDSPR model, the learning rates for both stages are set to 0.001, with a batch size of 36. In the first stage, the Stochastic Gradient Descent (SGD) optimizer with a momentum of 0.9 is employed. The trade-off parameters for the total loss, σ_1, σ_2, and σ_3, are set to 0.1, 0.5, and 0.07, respectively. Seven source domains are selected as combined source domains during domain selection with two statistical moments used to compute the central moment discrepancy (CMD). We use two statistical moments as a greater number does not improve the accuracy performance. In the second stage, the Adam optimizer is applied with hyperparameters ρ_1 and ρ_2 set to 0.1. We adopt a leave-one-subject-out cross-validation scheme. For the SEED dataset, only session 1 data is used as all three sessions share the same stimulus materials. For the SEED-IV dataset, accuracy and standard deviation are reported as the average across all three sessions. Ablation studies and Comparative Studies use the best-performing session from each dataset. Experiments are conducted on an NVIDIA GeForce GTX 4070 GPU using PyTorch 2.1.1 and Python 3.10.

Results

To comprehensively evaluate the performance of the proposed model, DDSPR is compared with other multi-source domain adaptation methods from existing studies. As summarized in Table 1, DDSPR achieves the highest average accuracy of 91.50% on the SEED dataset, accompanied by a standard deviation of 7.05%, marking an improvement of approximately 1% over the previously best-performing algo-

Table 1: Comparison of the performance results of different methods on the SEED and SEED-IV datasets.

Method	SEED	SEED-iV
	ACC/STD(%)	ACC/STD(%)
MS-MDA	80.62/11.03	57.92/10.12
MSMRA	83.62/09.58	69.77/07.37
UDDA	88.10/06.54	73.14/09.43
MS-ADA	86.16/07.87	59.29/13.65
MSGDAN	89.80/03.40	74.70/08.30
SH-MDA	90.27/05.56	73.41/08.27
DDSPR	**91.50/7.05**	**78.05/13.56**

rithm. For the SEED-IV dataset, we compare the average accuracy across three sessions. As shown in Table 1, DDSPR achieves an average accuracy of 78.05%, surpassing the highest accuracy reported in related studies. These results highlight the exceptional performance of DDSPR in cross-subject EEG emotion recognition tasks, demonstrating its effectiveness and robustness.

Ablation Study

The effectiveness of the DDSPR model is validated through ablation experiments. Table 2 presents the accuracy across all subjects in the best session of SEED (session 1) and SEED-IV (session 2) after removing key components of the proposed method.

Table 2: Ablation study on the SEED and SEED-IV datasets.

Method	ACC/SEED	ACC/SEED4
DDSPR	**91.50 ± 07.05**	**82.63 ± 10.70**
w/o ADAS	90.89 ± 06.83	79.12 ± 10.32
w/o DDS+ADAS	89.17 ± 07.21	77.32 ± 10.87

To assess the contribution of the Agent Domain Adaptation Strategy (ADAS), we observe that excluding ADAS reduces the model's accuracy from 91.5% to 90.89% on SEED and from 82.63% to 79.12% on SEED-IV. This highlights ADAS's role in enhancing source domain consistency and strengthening the model's domain selection capability.

The Dynamic Domain Selection (DDS) module, which mitigates negative transfer and improves classification performance, also plays a critical role. Removing DDS leads to a more pronounced accuracy drop, from 90.89% to 89.17% on SEED and from 79.12% to 77.32% on SEED-IV. These results demonstrate that DDS effectively reduces the impact of dissimilar source domains on model training and stability, further validating its importance within the proposed framework.

Comparative Study

To evaluate the effect of selecting different numbers of source domains in the dynamic domain selection module, we conduct a comparative analysis. Figure 3 illustrates the variation in model accuracy based on the number of combined source domains selected during the dynamic domain selection process. On the SEED dataset (session 1), the model achieves its highest accuracy of 91.50% when seven source domains are selected. A downward trend is observed as the number of source domains decreases, with fluctuations in accuracy. Conversely, increasing the number of selected source domains beyond seven results in a significant decline in performance. A similar pattern is evident on the SEED-IV dataset (session 2), where the accuracy peaks at 82.63% when seven source domains are selected. The observed trends across both datasets strongly indicate that selecting seven source domains as the combined source domains yields optimal performance.

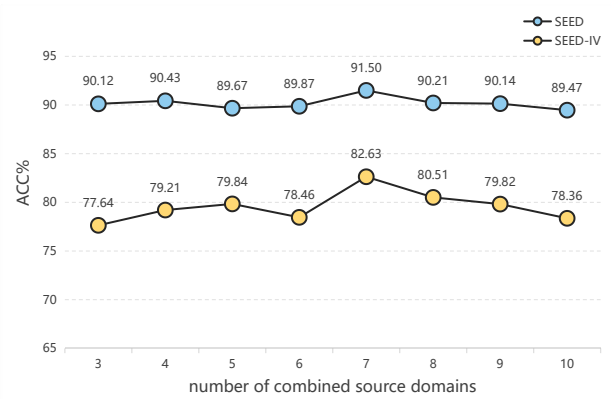

Figure 3: Compare the accuracy impressions of the combined source domains with different total subjects.

DISCUSSION AND CONCLUSION

In this paper, we present a DDSPR model to address the challenges posed by dissimilar source domains in multi-source domain adaptation for EEG-based emotion recognition tasks. The dynamic domain selection (DDS) module identifies source domains most similar to the target domain and combines them for adaptation. To complement DDS, the Agent Domain Adaptation Strategy (ADAS) is introduced, enhancing the model's generalization to source domains and indirectly improving its domain selection capability. Additionally, a pseudo-label correction strategy is employed to optimize high-confidence pseudo-labels, thereby enhancing emotion recognition performance in cross-subject tasks. Our model demonstrates superior results on two public emotion recognition datasets, SEED and SEED-IV. For future work, we plan to explore more advanced domain selection methods to further optimize source domain selection. Furthermore, we aim to refine the pseudo-label correction strategy by improving intra-class consistency and inter-class separability, ultimately enhancing the model's ability to distinguish between different emotional states. In addition,we plan to explore potential challenges of modeling in clinical or educational scenarios.

Acknowledgments

This work was supported by the Natural Science Foundation of China (62374121,61974109).

References

Bashivan, P., Rish, I., Yeasin, M., & Codella, N. (2015). Learning representations from eeg with deep recurrent-convolutional neural networks. *arXiv preprint arXiv:1511.06448*.

Cao, J., He, X., Yang, C., Chen, S., Li, Z., & Wang, Z. (2022). Multi-source and multi-representation adaptation for cross-domain electroencephalography emotion recognition. *Frontiers in Psychology*, *12*, 809459.

Chen, H., Jin, M., Li, Z., Fan, C., Li, J., & He, H. (2021). Ms-mda: Multisource marginal distribution adaptation for cross-subject and cross-session eeg emotion recognition. *Frontiers in Neuroscience*, *15*, 778488.

Dolan, R. J. (2002). Emotion, cognition, and behavior. *science*, *298*(5596), 1191–1194.

Ganin, Y., Ustinova, E., Ajakan, H., Germain, P., Larochelle, H., Laviolette, F., ... Lempitsky, V. (2016). Domain-adversarial training of neural networks. *Journal of machine learning research*, *17*(59), 1–35.

Goodfellow, I., Bengio, Y., Courville, A., et al. (2016). *Deep learning* (Vol. 521). MIT Press.

Gretton, A., Borgwardt, K. M., Rasch, M. J., Schölkopf, B., & Smola, A. (2012). A kernel two-sample test. *Journal of Machine Learning Research*, *13*, 723–773.

Gu, X., Sun, J., & Xu, Z. (2020). Spherical space domain adaptation with robust pseudo-label loss. In *Proceedings of the ieee/cvf conference on computer vision and pattern recognition* (pp. 9101–9110).

Jayaram, V., Alamgir, M., Altun, Y., Scholkopf, B., & Grosse-Wentrup, M. (2016). Transfer learning in brain-computer interfaces. *IEEE Computational Intelligence Magazine*, *11*(1), 20–31.

Li, J., Qiu, S., Shen, Y.-Y., Liu, C.-L., & He, H. (2019). Multisource transfer learning for cross-subject eeg emotion recognition. *IEEE transactions on cybernetics*, *50*(7), 3281–3293.

Li, Z., Zhu, E., Jin, M., Fan, C., He, H., Cai, T., & Li, J. (2022). Dynamic domain adaptation for class-aware cross-subject and cross-session eeg emotion recognition. *IEEE Journal of Biomedical and Health Informatics*, *26*(12), 5964–5973.

Musha, T., Terasaki, Y., Haque, H. A., & Ivamitsky, G. A. (1997). Feature extraction from eegs associated with emotions. *Artificial Life and Robotics*, *1*(1), 15–19.

Rahman, T., Ghosh, A. K., Shuvo, M., & Rahman, M. M. (2015). Mental stress recognition using k-nearest neighbor (knn) classifier on eeg signals. In *Int. conf. materials, electronics & information engineering (icmeie)* (pp. 1–4).

Salimnia, A. H. (2023). *Attention-based multi-source-free domain adaptation for eeg emotion recognition* (Unpublished master's thesis). The University of Western Ontario (Canada).

She, Q., Zhang, C., Fang, F., Ma, Y., & Zhang, Y. (2023). Multisource associate domain adaptation for cross-subject and cross-session eeg emotion recognition. *IEEE Transactions on Instrumentation and Measurement*, *72*, 1–12.

Shu, R., Bui, H., Narui, H., & Ermon, S. (2018). A dirt-t approach to unsupervised domain adaptation. In *International conference on learning representations (iclr)*.

Teplan, M., et al. (2002). Fundamentals of eeg measurement. *Measurement science review*, *2*(2), 1–11.

Wang, F., Zhang, W., Xu, Z., Ping, J., & Chu, H. (2021). A deep multi-source adaptation transfer network for cross-subject electroencephalogram emotion recognition. *Neural Computing and Applications*, *33*, 9061–9073.

Wang, J., Ning, X., Xu, W., Li, Y., Jia, Z., & Lin, Y. (2024). Multi-source selective graph domain adaptation network for cross-subject eeg emotion recognition. *Neural Networks*, *180*, 106742.

Wang, X.-W., Nie, D., & Lu, B.-L. (2011). Eeg-based emotion recognition using frequency domain features and support vector machines. In *Neural information processing: 18th international conference, iconip 2011, shanghai, china, november 13-17, 2011, proceedings, part i 18* (pp. 734–743).

Wu, X., Ju, X., Dai, S., Li, X., & Li, M. (2024). Multi-source domain adaptation for eeg emotion recognition based on inter-domain sample hybridization. *Frontiers in Human Neuroscience*, *18*, 1464431.

Xie, S., Zheng, Z., Chen, L., & Chen, C. (2018a). Learning semantic representations for unsupervised domain adaptation. In *International conference on machine learning (icml)* (pp. 5419–5428).

Xie, S., Zheng, Z., Chen, L., & Chen, C. (2018b). Learning semantic representations for unsupervised domain adaptation. In *International conference on machine learning* (pp. 5423–5432).

Yan, K., Kou, L., & Zhang, D. (2017). Learning domain-invariant subspace using domain features and independence maximization. *IEEE transactions on cybernetics*, *48*(1), 288–299.

Yang, L., & Liu, J. (2019). Eeg-based emotion recognition using temporal convolutional network. In *2019 ieee 8th data driven control and learning systems conference (ddcls)* (pp. 437–442).

Zeng, H., Li, X., Borghini, G., Zhao, Y., Aricò, P., Di Flumeri, G., ... Babiloni, F. (2021). An eeg-based transfer learning method for cross-subject fatigue mental state prediction. *Sensors*, *21*(7), 2369.

Zheng, W.-L., Liu, W., Lu, Y., Lu, B.-L., & Cichocki, A. (2018). Emotionmeter: A multimodal framework for recognizing human emotions. *IEEE transactions on cybernetics*, *49*(3), 1110–1122.

Zheng, W.-L., & Lu, B.-L. (2015). Investigating critical frequency bands and channels for eeg-based emotion recog-

nition with deep neural networks. *IEEE Transactions on autonomous mental development*, *7*(3), 162–175.

Zuo, Y., Yao, H., & Xu, C. (2021). Attention-based multi-source domain adaptation. *IEEE Transactions on Image Processing*, *30*, 3793–3803.